

Numerical Study of Winter Shamal Wind Forcing on the Surface Current and Wave Field in Bushehr's Offshore Using MIKE21

Mohammad Pakhirehzan¹, Maryam Rahbani^{2*}, Hossein Malakooti³

¹ Ph.D. student, Faculty of Marine Science and Technology, University of Hormozgan, Bandar Abbas, IRAN; mht_pa@yahoo.com

^{2*} Assistant Prof., Faculty of Marine Science and Technology, University of Hormozgan, Bandar Abbas, IRAN; maryamrahbani@yahoo.com

³ Associate Prof., Faculty of Marine Science and Technology, University of Hormozgan, Bandar Abbas, IRAN; hos_malakooti@yahoo.com

ARTICLE INFO

Article History:

Received: 11 Jun. 2018

Accepted: 18 Sep. 2018

Keywords:

Persian Gulf
winter Shamal wind
MIKE21

ABSTRACT

Marine areas are affected by different atmospheric phenomena such as wind and storm. In this research the effect of a large scale atmospheric phenomenon, known as Winter Shamal Wind, is investigated on the regime of currents and waves in the northwest part of the Persian Gulf. This wind normally occurs for the period of three to seven days, during December to early March. MIKE21 Coupled Model FM was applied to study the pattern of current and waves for this period. To provide the hydrodynamic data for the model and validate the simulated results, the wind data of ECMWF and mast meteorology of coastal synoptic station of Bushehr and wave data of buoy located offshore of Bushehr was used. The results indicated only a slight increase in current speed with no significant change in current direction during Winter Shamal Wind, showing a stable current pattern in northwest of the Persian Gulf. The significant wave height and wave propagation speed for the period of Winter Shamal Wind in comparison with the days prior to the wind show significant changes. The maximum wave speed in the area under investigation reaches up to 1 m/s and the significant wave height is almost 1 meter higher than that of normal situation.

1. Introduction

The Persian Gulf is one of the most important water ways in the world. It is also the center of the richest oil resources of the world (Kampf and Sadrinasab, 2006). This Gulf is semi enclosed shallow water with the average depth of about 35 m (Azizpour et al., 2014; Thoppil and Hogan, 2010a). Its total coastline is about 3000 km., of which about 1722 km is under the territory of Iran. The mean length of this Gulf is about 1000 km, its width reaches up to 336 km at its widest area, and its depth reaches up to about 90 m at the Strait of Hormuz. The Persian Gulf is connected to the Gulf of Oman and open oceans via Strait of Hormuz (Reynolds, 1993). The direction of the winds in the Persian Gulf is mainly northwesterly throughout the year. They are mostly stronger during November to February and weaker during the June to September (Thoppil and Hogan, 2010a).

This Gulf is stretched between latitudes 24°-30° N and longitudes 48°-58° E. Its climate therefore, can be divided into two seasons and two transitional periods.

Summer season starts from June and continues till September. This is followed by the autumn transition from October to November. Afterwards, December to March are known as the winter season, which is completed by the spring transition from April to May (Walters and Sjoberg, 1998).

Due to its geographical location, this Gulf is dominated by the monsoon known as Shamal wind. Shamal Wind is a climatic regime which is developed over Mediterranean Sea and extended to the Persian Gulf. It causes uneven weather conditions such as dust storms, and low level winds (Rao et al., 2003).

Shamal Wind is the only persistently strong wind in the Persian Gulf region that can last for several days with the winds which can reach strong to gale force over the open sea and routinely produce wind waves of 3–4 m high (Glejin, 2013).

The prevalent direction of the Shamal Wind is north and northwesterly (Al Senafi and Anis, 2015; Perrone, 1979). For northwesterly winds of the Persian Gulf, the plume from Shatt-al-Arab first heads towards the

Iranian coast and then spreads southeastward (Pous et al., 2013). This wind is categorized as Winter and Summer Shamal Wind. Summer Shamal Wind normally occurs between May and July, sometimes elongates till September. This wind is in connection with the interaction of thermal and seasonal climatic systems of low altitude which works over northwest India, Pakistan, Iran and Saudi Arabian high pressure. It is almost moderate wind with mean velocity of about 3 m/s (Rao et al., 2001).

Winter Shamal Wind (WSW) on the other hand, is a short term phenomenon, and can be categorized into two different types according to its persistence; one with the duration of about 1 to 3 days, and the other with the duration of about 3 to 5 days (Abdi et al., 2012). WSW can occur 3 times per year especially by the end of December and the beginning of the March (Rao et al., 2001). It occurs when a transient low pressure front conjunct with a cold and strong passing front of the Turkey's mountains. The front edge of the cold air mass carries near surface dusts, which could cause dust storm. This wind is stronger than Summer Shamal Wind. The near surface velocity of this wind, entering to the center of the Persian Gulf, is about 15 to 20 m/s. According to Thoppil and Hogan (2010b) velocity is about 5 times stronger than its initial velocity.

Since the oceans and coastal waters are bounded by the atmosphere, every near surface atmospheric phenomena can disturb their hydrodynamic and cause the onward, upward or downward movement of ocean (Stewart, 2008). The Persian Gulf, like every other coastal waters is supposed to be affected significantly by the WSW. There are numerous literatures published with this regard such as Rao et al. (2001); and Thoppil and Hogan (2010b). There are however, little review about the effect of this large scale wind system on the dynamic of the daily waves and currents in this Gulf.

Considering the northwestern part of the Persian Gulf, which is most affected by the Winter Shamal wind, the aim of this research was to study the hydrodynamic of the area due to WSW. Due to the lack of field measurements and in situ observations in many regions, nowadays numerically simulated wave data are widely used as the data bank for extracting designed wave characteristics and for further studies with this regard (Moieni et al., 2010). The employed measured wind data was those recorded at mast meteorology of coastal synoptic station of Bushehr. They are recorded at the height of 10 m and are proper to use as initial condition of the model.

The aim of this research is to simulate wave and current pattern of the area under the effect of WSW. For this reason a numerical model should be selected.

The most vital points to achieve a right decision is the applicability of that model in the area. Another point to choose a proper model is availability of input data should be feed to that model (Arı Güner et al., 2013).

Since MIKE21, developed by Denmark Hydraulic Institute (DHI), has been used successfully in different investigations area, the use of it has been considered appropriate for this study. The availability of the input data to feed to this model is also guaranteed.

2. Materials and Methods

2.1. Circulation in the Persian Gulf

As mentioned, the most investigations carried out in the Persian Gulf are focused on the main circulation in the Persian Gulf, or specifically in the Strait of Hormuz. Observations and field measurement of water properties and circulation in the Persian Gulf are limited in some temporal and spatial measuring field coverage (Yao, 2008). Surface current in the Strait of Hurmoz is always inward to the Persian Gulf (Sadrinasab, 2010) and this current continues through the Gulf to the end of the Gulf at the northeast, where this current is divided into two parts to flow along shores in the opposite direction of the main current (Fig 1).

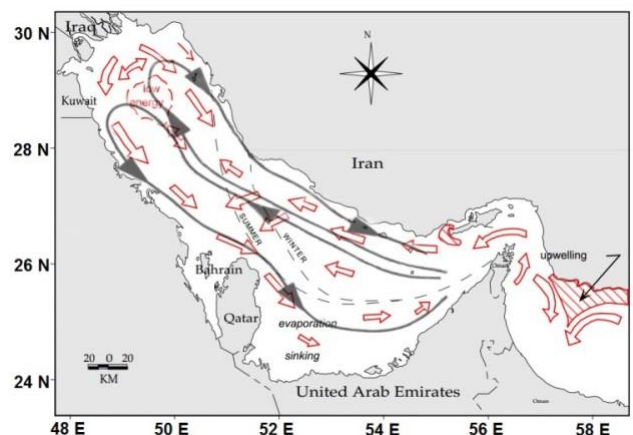


Figure 1. General circulation in the Persian Gulf (Pous et al. 2013, Reynolds 1993)

In a research by Kampf and Sadrinasab (2006), a three dimensional hydrodynamic model of the Persian Gulf was developed using Coherence software to study the full circulation through the Gulf. They claimed that the Gulf experiences two different cyclones; a cyclonic overturning circulation during spring and summer, and mesoscale eddies during autumn and winter.

Circulation in the Persian Gulf is divided into two different scales; the basin scale and mesoscale circulations. The basin scale in this Gulf is a cyclonic circulation; composed of a northwestward-flowing Iranian Coastal Current (ICC) from the Strait of Hormuz along the northern side of the basin with speeds greater than 10 cm/s and a southeastward-flowing current in the southern portion of the Gulf (Hunter, 1983; Thoppil and Hogan, 2010a). This basin scale of the Gulf is well known, due to the availability of vast literatures with this regard (Thoppil and Hogan, 2010a).

The surface current in this circulation is strong during the summer (reaches up to 20 cm/s), and is relatively weak during the winter (about 5 to 10 cm/s). The weakness of the current during winter is a result of the reduced density gradient between the Persian Gulf and the Gulf of Oman, which itself is due to the weak stratification at this time owing to the winter cooling (Thoppil and Hogan, 2010a). The strength of the cycle in the summer however, was suggested to be due the strengthening of stratification and weakening of the Shamal wind. Its magnitude reaches up to 40 cm/s. Besides, the isopycnals inclining downward toward the north is responsible for the strong long shore current. Details of the interior circulation during summer is barely known. The basin scale can be disturbed by three or four mesoscale eddies with the diameter of about 115-130 m, which are called as Iranian Coastal Eddies (ICE). These eddies extend down to the depth and also remain stationary at their locations. These eddies diminish as soon as the winter cooling cause the collapse of the thermocline (Thoppil and Hogan, 2010a).

2.2. Shamal Wind

Shamal Wind is a strong northwesterly wind which blows over a wide area of Iraq and Persian Gulf and spread out over Saudi Arabia and Kuwait. This wind is quite strong during the day, usually slows down during the night. It happens a few times per year; mostly in summer, but sometimes in winter. The sands brought up from Syria and Jordan by this wind causes strong sand storm in Iraq (El-Baz, 1994).

Shamal wind in general, is divided into two types; the Summer Shamal Wind, and the Winter Shamal Wind (WSW). The synoptic conditions relevant to the pressure variation between the high pressure of the Northern Arabian Peninsula, Iraq and the Mediterranean Sea in one hand, and the low pressure of southern Iran and the southern Arabian Peninsula in another hand are favorable conditions for the formation of the Shamal Wind. According to Rao et al. (2001) the days in which the surface wind direction is northwesterly or northerly and the hourly mean wind speed is 17 kn (8 m/s) or more for at least three hours a day, is called Shamal day.

The Summer Shamal Wind is more famous in the area than the Winter Shamal Wind. It is also known as 120 Days Wind. It affect the region predominantly during May to July and are known to be linked with the seasonal thermal low pressure lying over north-west India, Pakistan, Iran and southern Saudi Arabia. The WSW however, is the resultant of a permanent high pressure over the Saudi Peninsula after a cold front passage. It is directly associated with mid-latitude disturbances moving from west to east and is caused by the presence of a large pressure gradient that develops after a cold front passage. Upper level subsidence in associate with rapid formation of high pressure over

Saudi Arabia and Iraq reinforces the low-level northwesterly winds (Thoppil and Hogan, 2010b). This wind normally happens several times during November till March; sometimes with the short period of 24 to 36 hours and sometimes with the longer period of 3 to 5 days. Fig 2 depicts the influence of the WSW on the air characteristics of the area under investigation during the January 2013. It can be seen that WSW is started on the 10th of the January with the speed of over 40 km/h and lasts for 5 days.

The occurrence of the WSW from 10th to 16th of January 2013 is shown in Fig 2. Prevailed north and northwesterly winds during this period is clearly observable (Fig 2d). Besides, wind speed experiences its highest value in comparison with the other days of the month (Fig 2c). The drop of the barometric pressure (Fig 2b) and the air temperature (Fig 2a) at the beginning of the WSW approve the passage of the cold front. It also can be seen that during this 5 days period the drop of the temperature is in coincidence with an increase of temperature difference between the dew point and the air, which suggests the dryness of the area during WSW (Fig 2a). These findings are also reported by other scientists, among them Rao et al. (2001); Rao et al. (2003); and Thoppil and Hogan (2010a).

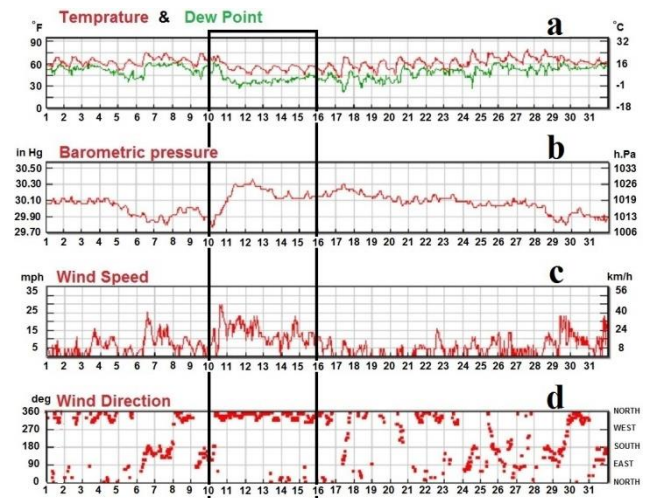


Figure 2. Temperature (a), pressure (b), wind speed (c) and wind direction (d) recorded at Bushehr station, January 2013- the black box shows the during the WSW (10th to 16th of January)- Bushehr meteorological station

2.3. Area under investigation

Bandar-e-Bushehr located in the northwest of the Persian Gulf, is a coastal city and an important port in Iran. This city can be counted as a relatively crowded port in terms of commercial and fishing activities. These activities are usually disturbed due to the WSW. Therefore, this specific area has been selected to investigate the effect of WSW on the hydrodynamic of its coastal body of water. The region has been considered for this investigation covers an area of about 9600 km², between longitudes 050° 00' E and 051° 07' E, and latitudes 28° 30' N and 29° 30' N. The deepest

part of the region is about 56 m, located on the southwestern part of the area (Fig 3).

Fig 4 shows the water level time series (A) and the wind rose (B) recorded at Bushehr meteorological station during January 2013. The geographical position of the buoy is: 28° 53' N, 050° 43' E. It can be seen that the wind is mostly northerly and northwesterly with the speed exceeds to 14 m/s. The figure also shows that semidiurnal tide is dominated in the area, with the tidal range of about 2 m. The horizontal line of zero water levels shows the chart datum of the Persian Gulf.

2.4. Model establishment

The two dimensional feature of the MIKE21 software has been adapted for this study. The software considers continuity, momentum, temperature, salinity and density equations for simulation. It is capable of simulating water level, flow and/or wave in the entrance of rivers, interior of gulfs, coastal areas and all other shallow and/or deep waters. The Flow module (FM) and the Spectrum Wave module (SW) of the software are adapted to use in this investigation. The ability of the software to execute coupled flow and wave module makes it suitable to perform the real situation.

Equations 1 to 3 are the conservation of mass and momentum equations which is used in this software to simulate the variation of the water level and the flow (DHI 2012).

$$\frac{\partial \zeta}{\partial t} + \frac{\partial p}{\partial x} + \frac{\partial q}{\partial y} = \frac{\partial D}{\partial t} \quad (1)$$

$$\begin{aligned} \frac{\partial p}{\partial t} + \frac{\partial}{\partial x} \left(\frac{p^2}{h} \right) + \frac{\partial}{\partial y} \left(\frac{pq}{h} \right) + gh \frac{\partial \zeta}{\partial x} \\ + \frac{gp\sqrt{p^2 + q^2}}{c^2 \cdot h^2} \\ - \frac{1}{\rho_w} \left[\frac{\partial}{\partial x} (h\tau_{xx}) + \frac{\partial}{\partial y} (h\tau_{xy}) \right] \\ - \Omega_q - fvv_x + \frac{h}{\rho_w} \frac{\partial}{\partial x} (\rho_a) = 0 \end{aligned} \quad (2)$$

$$\begin{aligned} \frac{\partial q}{\partial t} + \frac{\partial}{\partial y} \left(\frac{q^2}{h} \right) + \frac{\partial}{\partial x} \left(\frac{pq}{h} \right) + gh \frac{\partial \zeta}{\partial x} + \frac{gq\sqrt{p^2 + q^2}}{c^2 \cdot h^2} \\ - \frac{1}{\rho_w} \left[\frac{\partial}{\partial y} (h\tau_{yy}) + \frac{\partial}{\partial x} (h\tau_{xy}) \right] \\ - \Omega_p - fvv_y + \frac{h}{\rho_w} \frac{\partial}{\partial xy} (\rho_a) = 0 \end{aligned} \quad (3)$$

In the above mentioned equations the relation between the water depth ($h(x,y,t)$), the variation of water level with time ($d(x,y,t)$), and the water level ($\zeta(x, y, t)$) are related as follow:

$$h(x,y,t) = d(x,y,t) - \zeta(x,y,t) \quad (4)$$

The symbols used in the above equations are introduced in Table 1.

The spectral wave module (SW) simulates the growth, decay, and transformation of wind generated waves and swells in offshore and coastal areas. The waves in this module, are represented by the density spectrum $N(\sigma, \theta)$. The independent parameters are the relative angular frequency ($\sigma = 2\pi f$), and the direction of wave propagation (θ). The governing equation is the wave action balance equation formulated in either Cartesian or spherical co-ordinates (Komen 1996).

$$\begin{aligned} \frac{\partial N}{\partial t} + \nabla \cdot (\vec{v} N) = \frac{S}{\sigma} \\ \rightarrow \frac{\partial}{\partial t} N + \frac{\partial}{\partial x} C_x N + \frac{\partial}{\partial y} C_y N + \frac{\partial}{\partial \sigma} C_\sigma N + \frac{\partial}{\partial \theta} C_\theta N = \frac{S}{\sigma} \end{aligned} \quad (5)$$

where N is wave action density, σ is the relative angular frequency, θ is the wave direction, $C_x, C_y, C_\sigma, C_\theta$ are celerity characteristics in geographical and spectral coordinate system, and S is the energy source term, which represents the superposition of source function describing various physical phenomenon.

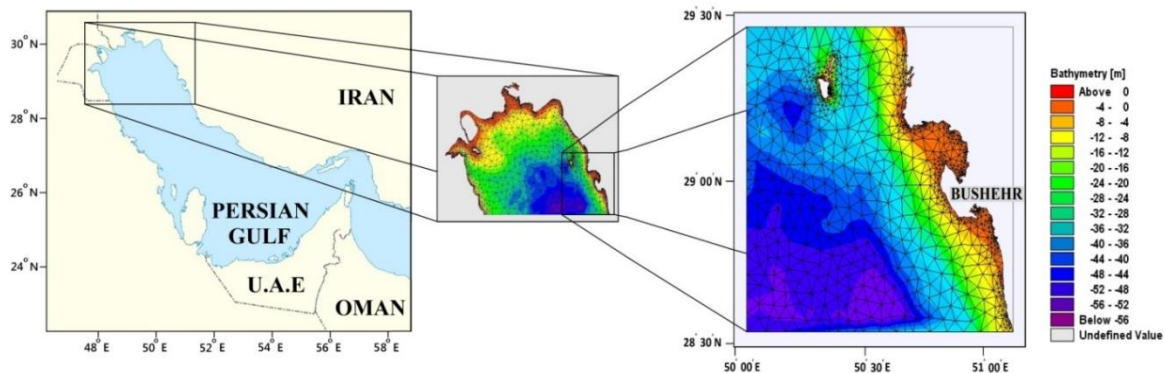


Figure 3. study area

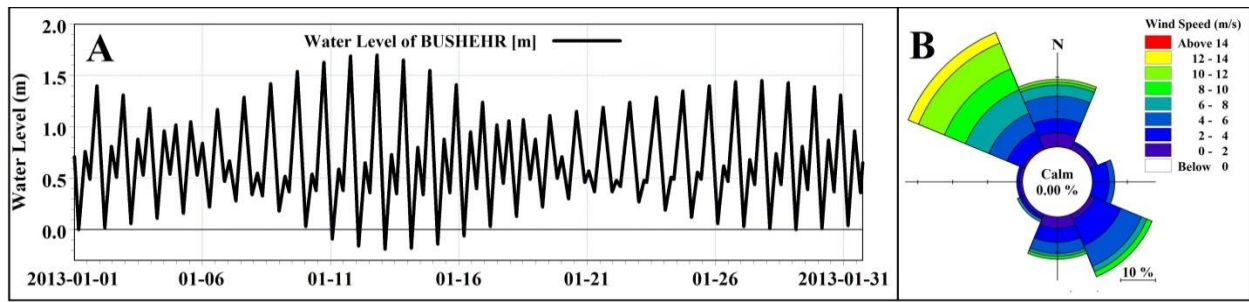


Figure 4. (A) Water level time series, and (B) Wind rose of the Busheher offshore –January, 2013

Table 1. Symbols used in equations

Phrase	Concept
$p, q(x, y, t)$	flux of density in the x and y direction
g	gravitational acceleration
$f(v)$	wind friction
$V(x)$	wind speed component in x direction
$V(y)$	wind speed component in y direction
$p_a(x, y, t)$	atmospheric pressure
ρ_w	water density
$\tau_{xx}, \tau_{xy}, \tau_{yy}$	shear stress components
t	time
$\Omega(x, y)$	Coriolis effect

$$S = S_{in} + S_{nl} + S_{ds} + S_{bot} + S_{surf} \quad (6)$$

where S_{in} represents the generated energy by the wind, S_{nl} is the wave energy transfer due to non-linear wave-wave interaction, S_{ds} is the dissipation of wave energy due to white capping, S_{bot} is the dissipation due to bottom friction and S_{surf} is the dissipation of wave energy due to depth-induced breaking (Remya 2014, Sorensen 2004).

The coupled feature of the software; SW and FM, has been adapted to simulate the surface current and also the significant wave height of the area before, during and after the WSW. The potency of simulating a phenomena considering simultaneous interaction between the flow and the wave of an area is the advantage of the usage of the coupled module. That is; the spectral wave tensions could be called directly from the SW to use in the FM module, on the other hand the variation of the water level can be reloaded from the FM module for the usage in the SW module.

For grid cells the flexible mesh has been adapted. The model has been established with the total number of the 2163 cells. The size of the grids varies from 0.5 km² in the area away from the coastal area, to about 0.1km² near the coast. The British Admiralty Nautical chart 2884 has been employed for the bathymetry of the area (Fig 3).

The wind speed and direction adapted to the model was those derived out from the ECMWF model. These data is recorded every 6 hours. The modeled area is bordered by three open boundaries at the north, east, and south, and one land boundary at the west. For the open boundary conditions the water level elevation was considered at all three open boundaries. These data are

collected from mobilegeographics web page. Water level data of Khark island station, and Boushehr station were applied for the northern, and southern boundaries respectively. For the eastern boundary the interpolation method between the northern and southern water level data was employed. Considering the geographical location of the area, and taking into account the selected period for simulation, the water temperature was set to 15°, and the water salinity was set to 39 ppt.

2.5. Model calibration and validation

Validation of the model was carried out using buoy recorded data and the ECMWF reanalysis databases for the interval 27th to 31st of January 2013. This period was considered for validation, since this period was the only interval, when the buoy records was available. Three main parameters has been used for the model calibration including white capping parameter, wave breaking parameter, and bottom friction parameter. The former played the main role in this calibration. Considering reconstructing the real situation, it was found necessary to consider white capping parameter as a small value. Executing several simulations, the value of $C_{ds}=2.5$ was found proper for white capping. For the wave breaking parameter the value of $\gamma=0.8$ has been choose. The bottom friction parameter was adapted to the model as Chezy coefficient. The smaller the Chezy coefficient, the bottom friction is much higher. Considering the speed of the current in the area and executing some simulations this parameter has been selected as 15.

Fig 5 shows the time series of wind speed, significant wave height and peak wave period derived out from calibrated model. The significant wave height and peak wave period of the simulation has been compared with buoy records and ECMWF data (b and c). As it can be seen the results of this model shows the good harmony with those of the buoy and ECMWF.

Since WSW ranges from January to March, according which, the wind speed and intensity increases, it affects the temperature and atmospheric pressure of the region. The best timing for the model simulation therefore, was considered to be from 10th to 16th of January (see Fig 2). The simulation was executed for longer period as a sake of comparison. Taking into account the proper Courant number, the time step for the simulation was selected as 300 seconds.

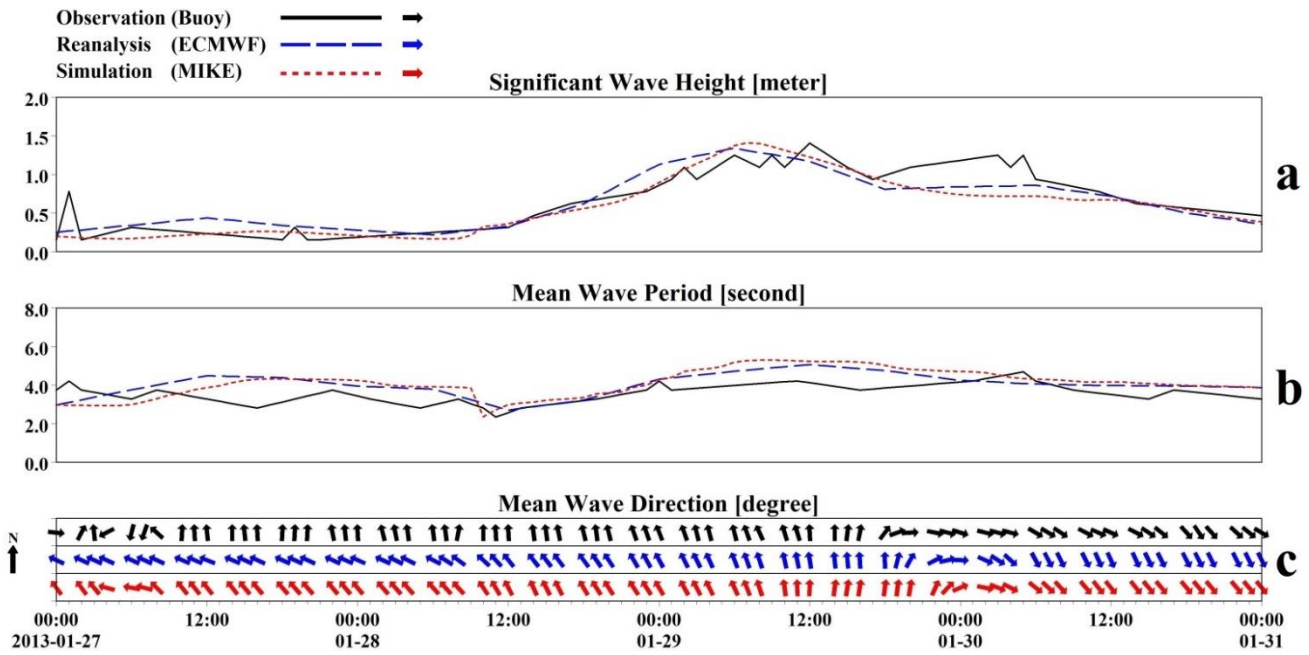


Figure 5. Time series of (a) significant wave height, (b) mean wave period, and (c) mean wave direction recorded in buoy, derived out from ECMWF reanalysed databasis, and from simulation applied in this study

In order to show statistically the goodness of results, and also to evaluate ECMWF data, four statistical parameters were considered including Bias, Correlation Coefficient (CC), Scattering Index (SI), and Root Mean Square Error (RMSE). These values are calculated for each model results and summarized in Table 2. According to these values, developed model in this research simulated wave parameters as good as the ECMWF reanalyzed databases; this is true for significant wave height, mean wave period, and mean wave direction. It should however be mentioned that simulated results represented by ECMWF shows slightly better agreement with buoy data in the case of significant wave height.

Table 2: Calculated statistical wave parameters

model	Wave parameters	Bias	CC	RMSE	SI
MIKE	Height	-0.065	0.90	0.17	0.27
	Period	0.53	0.59	0.77	0.21
	Direction	-15.9	0.88	37.3	0.17
ECMWF	Height	-0.005	0.91	0.16	0.26
	Period	0.46	0.55	0.67	0.18
	Direction	-20.04	0.86	48.3	0.23

3. Results and discussion

Figs 6 and 7 represent the time series data derived from the model. Fig 6 contains current speed and direction, and Fig 7 contains significant wave height, mean wave period and direction, for the period before, during and after WSW.

Fig 6 which show the time series of current speed and direction at monitoring point implies that WSW do not disturb the current speed and/or direction. Since the dominant current in the Persian Gulf is the result of tidal current, and current due to the density, this finding

was presumed. The simultaneous variation between the wind speed and significant wave height is clear in the Fig 7. The rise of significant wave height (7b) simultaneous with the beginning of WSW (7a) is clearly shown in the figure. Fig 7c shows that the mean wave period is increased at the beginning of WSW. And Fig 7d shows the main direction of the wave propagation at the monitoring point.

Fig 8 shows the pattern of current for the whole area under investigation for a time step before, during, and after the WSW derived out from simulation using MIKE21. The date and time when the plots have been derived out, is at high tide. Plots of surface current show that the WSW has almost no effect on the pattern of surface current in this area. The dominant current in the northwest of Persian Gulf, as mentioned by literatures, is from northwest toward southeast (Pous et al., 2013; Reynolds, 1993; Kampf and Sadrasab, 2006). The strength of the surface current is also almost the same for the three different periods.

The pattern of significant wave height for the area has been shown in Fig 9. The date and time when the plots have been derived out are: 17:00 in 9th of January (before WSW), 20:00 in 12th of January (During WSW), and 20:00 in 17th of January (after WSW). It is for a time step before, during, and after the WSW. Comparison of significant wave heights of the area for these three time steps shows significant effect of the WSW on the wave pattern of the area. It can be seen that this wind affects the height and the speed of the wave significantly. The wave height in the area is barely exceeds 1 m. before and after the wind, while during the WSW (middle plot) is mostly between 0.9 to 2.2m. This wind also causes the increase of the wave speed from about 1 m/s to about 2 m/s (almost twice).

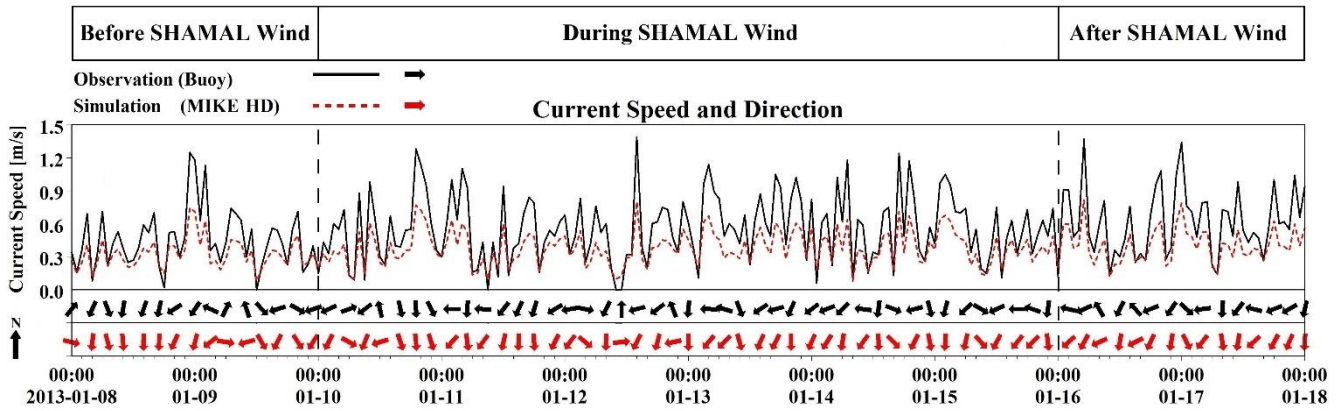


Figure 6. Time series of current speed and direction derived out from buoy data, and simulated by MIKE21 for the 08 to18 of January 2013

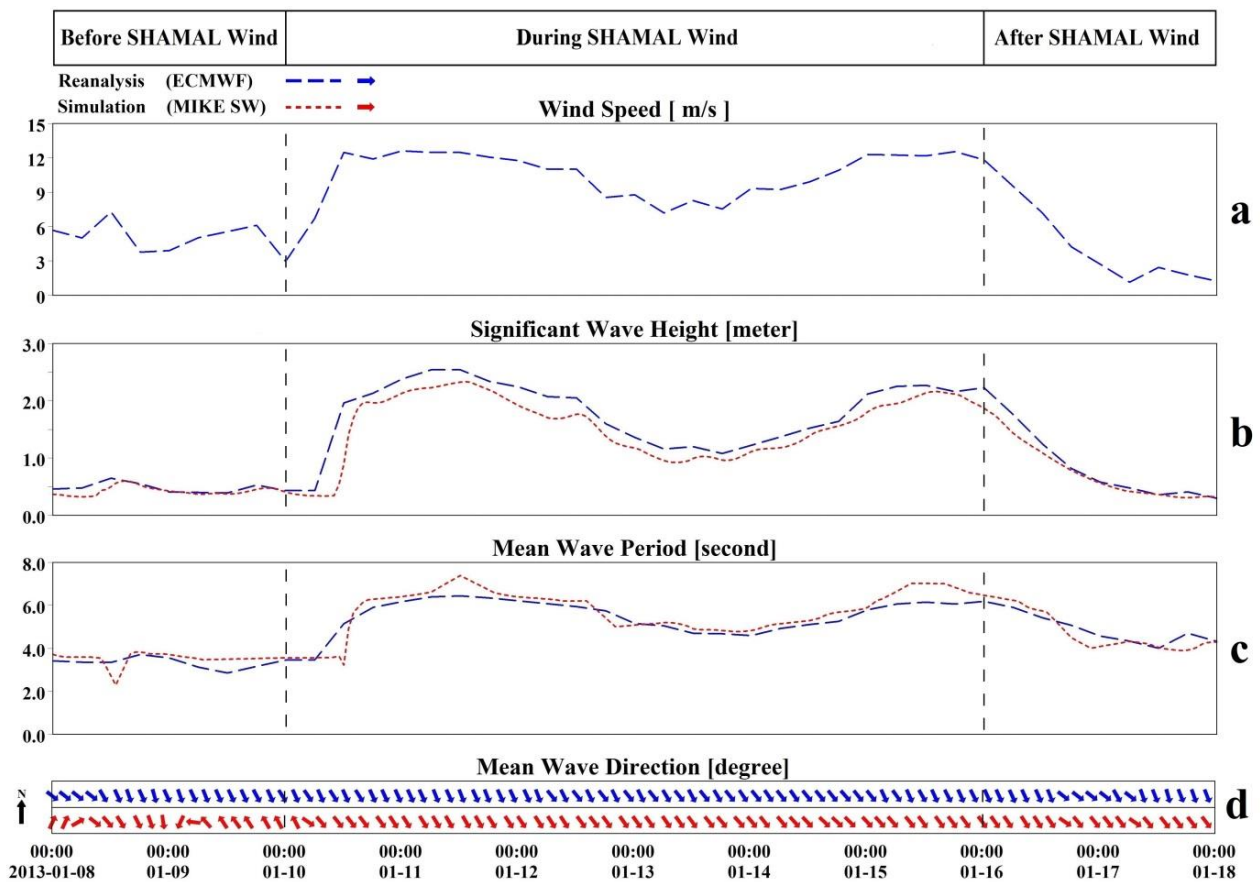


Figure 7. Time series of (a) Wind speed, (b) significant wave height, (c) mean wave period, and (d) mean wave direction of the simulation using MIKE21 in compare with ECMWF data, for the 08 to18 of January 2013

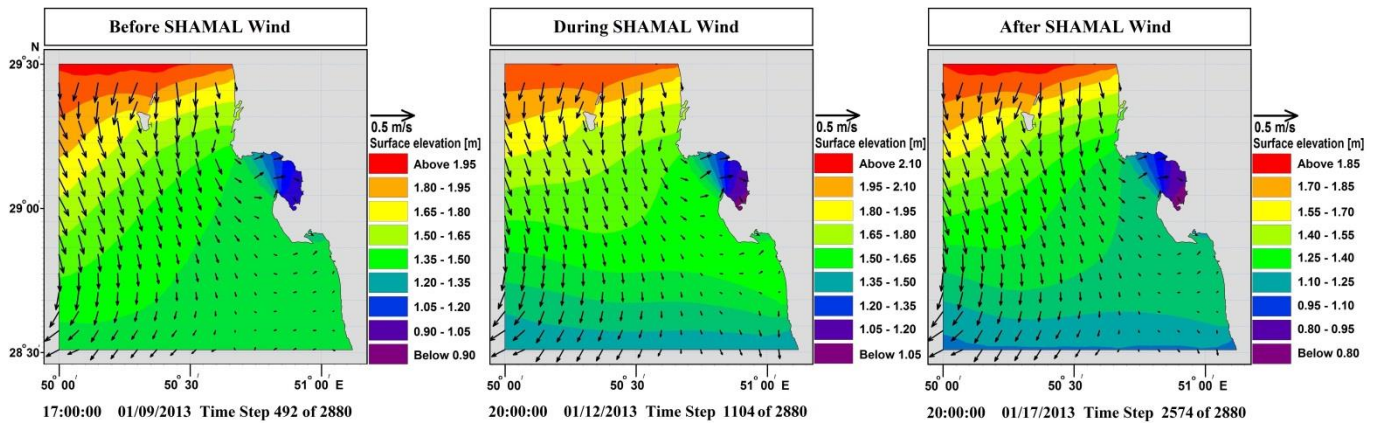


Figure 8. Patterns of current in the area under investigation for a time step before (top), during (mid), and after (down) WSW derived out from model

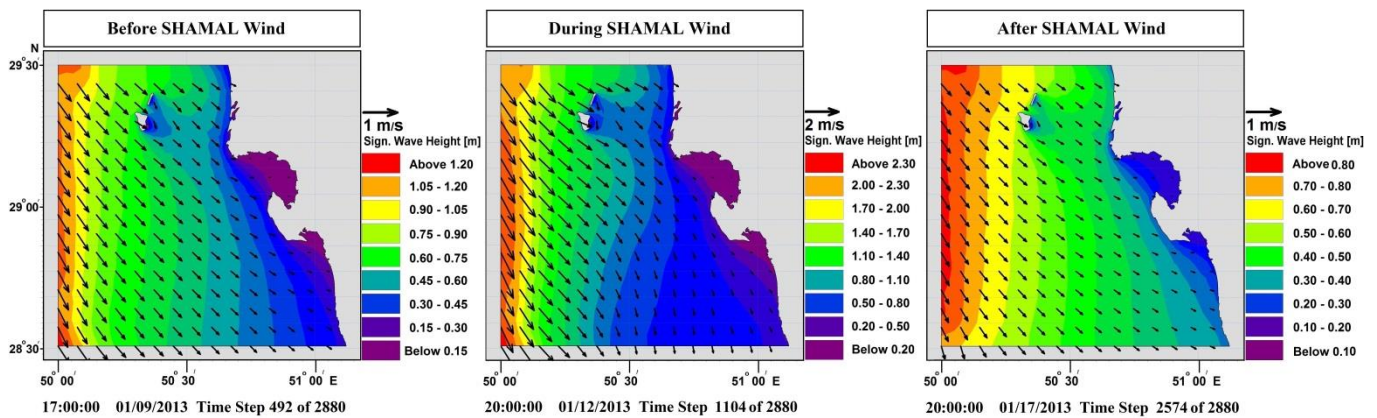


Figure 9. Patterns of significant wave height in the area under investigation for a time step before, during, and after WSW derived out from model

4. Conclusions

The effect of Winter Shamal Wind on the pattern of current and wind in the northwest of the Persian Gulf is studied using MIKE21. It was found that the direction of surface current in the study area is almost uniform and the simulated results shows no significant variety before, during and after the Winter Shamal wind. However, a small increase of about 0.1 m/s in speed of surface current was observed during Winter Shamal wind. Its direction is from the northwest to the southeast. It can be said that the pattern of current in the Persian Gulf as a semi-enclosed area always follows a general pattern of this Gulf and does not affected by Winter Shamal Wind.

In terms of significant wave height and wave speed however, results was different. Simulated results shows that During the Winter Shamal Wind, the maximum wave height is higher than that of before and after this wind. Moreover, it was found that the speed of waves exceeds to about 2 m/s during Winter Shamal Wind, which is a considerable amount for the wave speed.

The wave direction in the period of Winter Shamal Wind is mostly northerly and northwesterly. While, it is often southerly and easterly before and after the Winter Shamal Wind.

5. References

- 1- Abdi Vishkaee, F., Flamant, C., Cuesta, J., Oolman, L., Flamant, P., & Khalesifard, H. R (2012) Dust transport over Iraq and northwest Iran associated with winter Shamal: A case study. *Journal of Geophysical Research: Atmospheres*, 117(D3).
- 2- Al Senafi F, Anis A (2015) Shamals and climate variability in the Northern Arabian/Persian Gulf from 1973 to 2012. *International Journal of Climatology*, 35: 4509-4528.
- 3- Arı Güner H A, Yüksel Y, Özkan Çevik E (2013) Estimation of wave parameters based on nearshore wind–wave correlations. *Ocean Engineering*, 63: 52-62.
- 4- Azizpour, J., Chegini, V., Khosravi, M., & Einali, A (2014) Study of the physical oceanographic properties of the persian gulf, strait of hormuz and gulf of oman based on PG-GOOS CTD measurements. *Journal of the Persian Gulf*, 5(18): 37-48.
- 5- DHI. 2012. Mike21/3 Coupled Model FM, scientific documentation, D.H.I., Denmark.
- 6- El-Baz F (1994) The Gulf War and the environment. Taylor and Francis
- 7- Glejin, J., Kumar, V. S., Nair, T. B., Singh, J., & Mehra, P (2013) Observational evidence of summer Shamal swells along the west coast of India. *Journal of Atmospheric and Oceanic Technology*, 30(2): 379-388.

- 8- Hunter J R (1983) Aspects of the dynamics of the residual circulation of the Arabian Gulf. *Coastal Oceanography*, 31-42
- 9- Kampf J, Sadrinasab M (2006) The circulation of the Persian Gulf: a numerical study. *Ocean Science*, 2: 27-41.
- 10- Komen G J, Cavaleri L, Donelan M, et al (1996) *Dynamics and modelling of ocean waves*. Cambridge University Press
- 11- Moeini M H, Etemad-Shahidi A, Chegini V (2010) Wave modeling and extreme value analysis of the northern coast of the Persian Gulf. *Applied Ocean Research*, 32: 209-218.
- 12- Perrone T J (1979) Winter shamal in the Persian Gulf. *Naval environmental prediction research facility monterey ca*, 180 p.
- 13- Pous S, Carton X, Lazure P (2013) A Process Study of the Wind-Induced Circulation in the Persian Gulf. *Open Journal of Marine Science*, 03: 1-11.
- 14- Rao P G, Al Sulaiti M, Al Mulla A H (2001) Winter shamals in Qatar, Arabian Gulf weather. *Weather*, 56: 444-451.
- 15- Rao P G, Hatwar H R, Al Sulaiti M H, et al (2003) Summer shamals over the Arabian Gulf. *Weather*, 58: 471-478.
- 16- Remya P G, Kumar R, Basu S (2014) An assessment of wind forcing impact on a spectral wave model for the Indian Ocean. *Journal of Earth System Science*, 123: 1075-1087.
- 17- Reynolds R M (1993) *Physical oceanography of the Gulf, Strait of Hormuz, and the Gulf of Oman—Results from the Mt Mitchell expedition*. *Marine Pollution Bulletin*, 27: 35-59.
- 18- Sadrinasab M (2010) Three dimensional numerical modeling of the circulation in the Persian Gulf. *Oceanography*, 1: 19-24.
- 19- Sorensen L S (2004) A third-generation spectral wave model using an unstructured finite volume technique. In *29th Intern Conf on Coastal Eng. Asce American Society Of Civil Engineers*
- 20- Stewart R H (2008) *Introduction to physical oceanography*. Texas: Texas A and M University, 133-147
- 21- Thoppil P G, Hogan P J (2010a) A modeling study of circulation and eddies in the Persian Gulf. *Journal of Physical Oceanography*, 40: 2122-2134.
- 22- Thoppil P G, Hogan P J (2010b) Persian Gulf response to a wintertime shamal wind event. *Deep Sea Research Part I: Oceanographic Research Papers*, 57: 946-955.
- 23- Walters Sr K R, Sjoberg W F (1998) *The Persian Gulf region: a climatological study*. USA, USAF Environmental Technical Applications Center, Scott Air Force Base, Illinois, 62225-5438.
- 24- Yao F (2008) *Water mass formation and circulation in the Persian Gulf and water exchange with the Indian Ocean*. Coral Gables, Florida: University of Miami